ELSEVIER

Journal of Biomechanics 40 (2007) 476–480

JOURNAL OF BIOMECHANICS

www.elsevier.com/locate/jbiomech
www.JBiomech.com

Short communication

Studies of plasma membrane mechanics and plasma membrane–cytoskeleton interactions using optical tweezers and fluorescence imaging

Sergey A. Ermilov[a], David R. Murdock[a], Feng Qian[a], William E. Brownell[b], Bahman Anvari[a,*]

[a]*Department of Bioengineering, Rice University, P.O. Box 1892, MS 142, Houston, TX 77251-1892, USA*
[b]*Department of Otorhinolaryngology and Communicative Sciences, Baylor College of Medicine, Houston, TX, USA*

Accepted 4 December 2005

Abstract

We use optical tweezers in conjunction with an optical position-sensing system, which spectrally filters signals generated by a trapped fluorescent microsphere to study plasma membrane (PM) mechanics and its interactions with cytoskeleton. We dynamically measure the PM tethering force on human embryonic kidney cells that are a standard cultured cell line. Recorded tethering force vs. PM displacement profiles, revealed the tether formation process, initiated with linear deformation of the PM, followed by a nonlinear regime and terminated with the local separation of PM. Tethering force vs. displacement profiles were used to estimate tether formation force and stiffness parameter of the PM. Integration of the force–displacement profiles yielded the work of tether formation, including linear and nonlinear components. Our results demonstrate that spectral filtering of the optically trapped fluorescent microsphere image formed on the position-sensing system overcomes the artifacts introduced by the transillumination imaging and allows accurate measures of PM mechanics before and during the initial stages of tether formation.

Keywords: Laser trapping; Biological forces; Viscoelasticity; Stiffness; Tether

1. Introduction

Local mechanical properties of the plasma membrane (PM) and underlying supporting cytoskeleton, largely determine shape-change resistance of the cell, which is important for many biological processes, including deformation of erythrocytes in capillaries, electromotility of outer hair cells, cell division, phagocytosis, pseudopodium and dendritic spine formation. Single beam gradient force optical traps (optical tweezers) (Ashkin et al., 1986) provide an accurate technology to measure forces exerted on a trapped microsphere within the range of a few to several hundred piconewtons (Wright et al., 1994; Gauthier and Wallace, 1995; Brouhard et al., 2003). In this technique, the transverse displacement of a microsphere from the trapping center, linearly related to the transverse trapping force, is commonly measured using position-sensing device such as a quadrant photodetector (QPD). The transillumination mode of microsphere imaging on the QPD has been successfully used in studies of PM mechanics by pulling long (10–100 μm) PM tethers (Simmons et al., 1996; Mehta et al., 1998; Li et al., 2002). However, if the trapped microsphere is within proximity of the cell (about two microsphere radii or less), the cell image formed on the QPD contributes to a large optical artifact, introducing an error on the estimated mechanical parameters (Qian et al., 2004). A particular approach to overcome the problem of the cell image

*Corresponding author. Tel.: +713 348 5870; fax: +713 348 5877.
E-mail addresses: sermilov@fairwaymed.com (S.A. Ermilov), anvari@rice.edu (B. Anvari).
URL: http://www.ruf.rice.edu/~banvari/.

0021-9290/$ - see front matter © 2006 Elsevier Ltd. All rights reserved.
doi:10.1016/j.jbiomech.2005.12.006

artifacts is based on spectral separation of the images of the trapped microsphere and the cell. In this work we demonstrate the advantages offered by the use of optically trapped fluorescent microspheres for studies of cellular mechanics.

2. Methodology

The optical tweezers setup (Ermilov and Anvari, 2004) was combined with a fluorescence imaging system (Fig. 1). The light from a halogen light source was used for visualization of the cells and the trapped microsphere on the CCD camera. A band-pass filter (15) was used to allow the transmission of the visualizing light in the 450–510 nm spectral range through a dichroic mirror (8) with a transparency band between 360 and 510 nm towards a beam splitter. The beam splitter directed 10% of the light to the CCD camera, while the remaining 90% was blocked by a filter (21) with spectral band-pass of 605 ± 27.5 nm (Appendix 1 at http://www.elsevier.com/locate/jbiomech).

We optically trapped a 4 μm diameter sulfate-modified fluorescent polystyrene microsphere (F-8858, Molecular Probes, Eugene, OR) with excitation spectrum between 480 and 590 nm and maximum fluorescence emission at 605 nm. The fluorescence excitation light from a 75 W xenon short arc lamp was passed through an excitation band-pass (535 ± 25 nm) filter, and reflected by the dichroic mirror (8) towards the trapped fluorescent microsphere. The fluorescent light emitted from the trapped microsphere was split by the 1/9 beam splitter, with its largest portion spectrally separated from the visualizing light by the emission band-pass filter and directed towards a QPD (QP 1.1-6-TO18, Pacific Silicon Sensor, Westlake Village, CA).

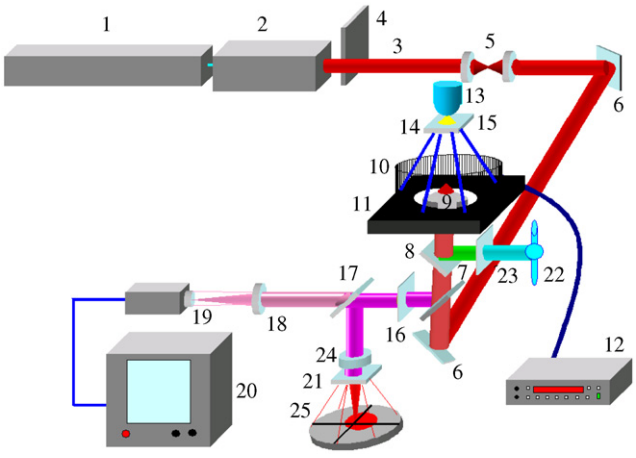

Fig. 1. Experimental setup. 1—Nd:YVO_4 laser ($\lambda = 532$ nm), 2—Ti:Sapphire laser ($\lambda = 830$ nm, 300 mW after microscope objective), 3—laser beam, 4—beam shutter, 5—collimating system, 6—mirror, 7—dichroic mirror (transmitting light with $\lambda > 650$ nm), 8—dichroic mirror (transmitting light with $\lambda = 360-510$ nm and $\lambda > 565$ nm), 9—100×1.3 NA oil immersion microscope objective, 10—sample chamber, 11—PZT stage, 12—generator of control signals, 13—halogen visualization light source, 14—visualizing light, 15—band-pass filter (480 ± 30 nm), 16—IR filter (transmitting light with $\lambda < 705$ nm), 17—10/90 beam splitter, 18, 24—imaging lens, 19—CCD camera, 20—video monitor, 21—emission band-pass filter (605 ± 27.5 nm), 22—xenon fluorescence light source, 23—excitation band-pass filter (535 ± 25 nm), 25—quadrant photodetector.

Transverse trapping force calibration has been previously described (Ermilov et al., 2005). Viscosity of the normal extracellular solution (NES) (Ermilov et al., 2005), measured using a viscometer (Rheolyst AR 1000, TA Instruments, New Castle, DE) at shear rates between 10 and 100 s^{-1}, was 1.28 mPa s. We tested our technique by measuring mechanical properties of HEK-293 cells (Advanced Cell Technology, Worcester, MA) PMs, prepared as described by Ermilov et al. (2005) in sample chambers coated with an antimycotic solution in order to prevent microsphere adhesion (Appendix 2 at http://www.elsevier.com/locate/jbiomech).

A piezoelectric microscope stage (PZT) was used to bring the cell into contact with the trapped microsphere. After PM-microsphere contact, the cell was moved away at 1 μm/s speed for 10 s to form a PM tether. The PZT was subsequently stopped, and the relaxation of tethering force was recorded for 60 s.

We analyzed temporal tethering force profiles to obtain parameters related to the viscoelastic behavior of PM tethers (Fig. 2). Last 100 samples of the tethering force signal immediately prior to relaxation were averaged to estimate the steady-state tethering force (F_{ss}). The force relaxation part was analyzed using a bi-exponential model (Murdock et al., 2004), which yielded equilibrium tethering force (F_{eq}), two relaxation amplitudes (F_{short} and F_{long}) and two relaxation time

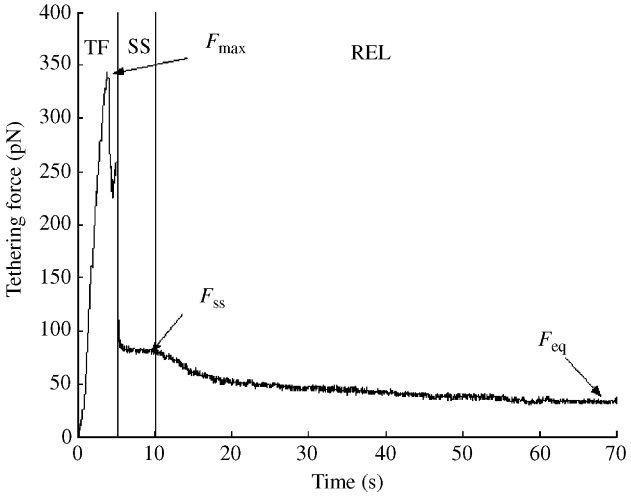

Fig. 2. Typical temporal PM tethering force profile, showing tether formation (TF), steady-state (SS), and relaxation (REL) segments for an HEK cell. F_{max}—TF force, F_{ss}—steady-state tethering force, F_{eq}—equilibrium tethering force.